Pergamon

Int. J. Heat Mass Transfer. Vol. 39, No. 2, pp. 275–288, 1996

0017-9310/96 $9.50+0.00

0017-9310(95)00136-0

Film boiling from a downward-facing curved surface in saturated and subcooled water

MOHAMED S. EL-GENK and ALEXANDER G. GLEBOV

Chemical and Nuclear Engineering Dept./Institute for Space and Nuclear Power Studies, University of New Mexico, Albuquerque, NM 87131, U.S.A.

(*Received* 20 *December* 1994 *and in final form* 13 *March* 1995)

Abstract—Film boiling from a downward-facing curved surface in saturated and 5 K, 10 K, and 14 K subcooled water was investigated experimentally. Local and surface average Nusselt number correlations developed for both saturation and subcooled conditions were within ±10% of data. Surface rewetting in saturation boiling was hydrodynamically driven, but thermally driven in subcooled boiling. Consequently, surface rewetting in the former occurred earlier at higher q_{min}; the critical film thickness prior to rewetting, however, was higher than that at 10 K and 14 K subcooling, but lower than at 5 K subcooling. Surface rewetting occurred first at lowermost position, $\theta = 0°$, then sequentially at higher inclinations. For saturation boiling, the critical film thickness was ~85 μm and 180 μm at $\theta = 0°$ and 8.26°, respectively. For subcooled boiling at $\theta = 0°$, the critical film thickness (~50 μm) was smaller; it increased, however, with increased inclination and decreased subcooling, reaching ~175 μm at $\theta = 8.26°$ and 5 K subcooling.

INTRODUCTION

Film boiling heat transfer from inclined, downward-facing flat surfaces [1–8] and on the inside or outside of curved surfaces is of interest in many fields. For example, film boiling on the inside of curved surfaces is important in thermal management of cryogenic liquids in ground storage tanks and for handling of storage tanks of hazardous and liquid chemicals during a fire. In these applications, it is desirable to achieve film boiling at low wall heat flux in order to avoid pressurization and explosive rupture of the tanks. Other applications include cooling of electric cables by pool boiling of liquid helium in superconductivity research and the telecommunication industry and passive cooling of the lower head of an advanced light water reactor pressure vessel by boiling in an underlying water pool following a core meltdown accident [9–11]. In these applications, knowledge of the maximum heat flux and the minimum film boiling surface heat flux (q_{min}), and corresponding wall superheats as well as of film boiling heat transfer is important for design purposes and for establishing operation and safety margins.

Film boiling from curved surfaces has not received much attention; only little work has been reported for inclined and downward-facing flat surfaces. Ishigai *et al.* [1] pioneered the work on film boiling from flat downward-facing flat circular copper plates, 25 and 50 mm in diameter, in saturated water. Jung *et al.* [2] and Seki *et al.* [3] investigated film boiling from upward-facing and downward-facing flat surfaces in saturated R-11; Seki *et al.* [3] for saturated R-11 at 2 bar. Seki *et al.* [3] reported that q_{min} for the downward-facing position was much lower than that for the upward-facing position. The film boiling heat flux values for R-11, however, were consistently lower than those for water, which Jung *et al.* attributed to the difference in physical properties of the two liquids. Neither Ishigai *et al.* nor Jung *et al.* reported values for q_{min} or corresponding wall superheats, $(\Delta T_{sat})_{min}$; only one value each was reported by Jung *et al.* [2] showed film boiling heat flux to increase with increased inclination angle from $\theta = 0°$ (downward-facing) to $\theta = 180°$ (upward-facing). The vapor film for downward-facing surfaces was much more stable than for inclined and upward-facing surfaces, delaying rewetting and resulting in much lower film boiling heat flux [2, 4, 5]. These investigations of film boiling from downward-facing and inclined flat surfaces [1–3] used steady-state heating and were only for saturation condition; few data is available for flat and inclined surfaces in subcooled water [4, 5].

Guo and El-Genk [4, 5] and El-Genk and Guo [6] performed quenching experiments using a flat inclined surface, 50.8 mm in diameter and 12.8 mm thick, in saturated and subcooled water (5, 10, 15 and 20 K subcooling) at θ of 0, 5, 10, 15, 30, 45 and 90° (vertical). The film boiling results agreed qualitatively with those in refs. [1–3]. The values of q_{min} and $(\Delta T_{sat})_{min}$ increased as liquid subcooling increased. These results as well as those of other investigators [1–3] are, however, not applicable to pool boiling from downward-facing curved surfaces, for which, to the best of the authors knowledge, there is very little experimental data available [7, 8].

Recently, El-Genk *et al.* [7] and El-Genk and Glebov [8] performed quenching experiments, which employed three copper sections of the same diameter (50.8 mm) and surface radius (148 mm), but of differ-

NOMENCLATURE

a, b	exponents, equations (3) and (10)
A	surface area [m^2]
B, C	coefficients, equations (2) and (29)
C_p	specific heat [kJ kg^{-1} K^{-1}]
D	diameter of test section [m]
f	frequency of vapor release [s^{-1}]
g	acceleration of gravity [9.81 m s^{-2}]
h	heat transfer coefficient [W m^{-2}K^{-1}]
h_{fg}	latent heat of vaporization [kJ kg^{-1}]
h'_{fg}	modified latent heat of vaporization, $\{h_{fg}+0.5C_{pv}\Delta T_{sat}\}$ [kJ kg^{-1}]
Ja	Jacob number, $C_{pv}\Delta T_{sat}/h'_{fg}$
k	thermal conductivity [W m^{-1}K^{-1}]
Nu	Nusselt number, $\{q\cdot D/(k_v\cdot\Delta T_{sat}\}$ or $(h\cdot D/k_v)$
q	surface heat flux [MW m^{-2}]
r	radial coordinate
Ra	Rayleigh number, $\{gD^3[\{\rho_l-\rho_v\}/\rho_v]/\nu_v\alpha_v\}$
R	radius [m]
t	time [s]
T	temperature [K]
V	volume [m^3].

Greek symbols

α	thermal diffusivity [m^2 s^{-1}]
δ	vapor film thickness [m]
$\Delta\delta$	amplitude of vapor film oscillations [m]
ΔT_{sat}	wall superheat $[T_w-T_{sat}]$ [K]
ΔT_{sub}	water subcooling $(T_{sat}-T_p)$ [K]
ε	emissivity
θ	local inclination [°]
ν	kinematic viscosity [m^2 s^{-1}]
ρ	density [kg m^{-3}]
σ	Stefan–Boltzmann constant $[5.669\times10^{-8}$ W m^{-2}K^{-4}]
τ	dimensionless time, $(t-t_0)/(t_{rew}-t_0)$.

Subscripts

B	released vapor from edge of boiling surface
c	critical
ev	evaporation at liquid–vapor interface
fB, f	film boiling, liquid
l	liquid
min	minimum film boiling
NC	natural convection
o	initial or at the beginning of quenching
p	water pool
rew	rewetting
R	radiation
s	curved surface
Sat	saturation
Sub	subcooled
v	vapor
w	boiling surface, wall.

Superscripts

$\bar{}$	surface average.

ent thicknesses (12.8, 20 and 30 mm). Local and average pool boiling curves were obtained for saturation and 5, 10 and 14 K water subcooling. The maximum and minimum film boiling heat fluxes, which increased with increased subcooling, were independent of wall thickness >19 mm and Biot number >0.8 and 0.008, respectively, indicating that boiling curves for the 20 and 30 mm thick sections were representative of quasi steady-state, but not those for the 12.8 mm thick section.

The objective of this work was to investigate film boiling heat transfer in the experiments of El-Genk and Glebov [8], using the data of the 20 mm thick section. Experimental data and video images of boiling surface were analyzed to determine: (a) the quenching mechanism of film boiling in saturation and subcooled boiling, (b) the effect of water subcooling on local film boiling heat flux, vapor film thickness, and rewetting time, and (c) q_{min}, $(\Delta T_{sat})_{min}$ and the critical film thickness, prior to surface rewetting, as functions of local inclination on the surface and water subcooling. The local and surface average Nusselt numbers were also correlated in terms of Rayleigh and Jacob numbers, for both saturation and subcooling conditions.

EXPERIMENTAL SETUP AND PROCEDURES

The experimental setup and procedures detailed in [7, 8], are only summarized herein. The copper section [Fig. 1(a)] had eight, K-type thermocouples (TC1–TC8) placed ~0.5 mm from the boiling surface, to provide temperature data for subsequent determination of the local and average pool boiling heat fluxes and surface temperatures in the various boiling regimes, and three thermocouples placed ~5 mm from the top surface (TC9–TC11). The copper section mounted in a water sealed Marinite C insulation mold was housed in a cylindrical Bakelite skull for additional insulation and handling. The Marinite mold and the Bakelite skull were machined at the surface to the same curvature as the boiling surface in order to avoid edge effects influencing the release of vapor [Fig. 1(a)].

The quenching tank had large glass windows on four sides for visual observation. To observe the entire boiling surface during quenching, a water sealed mirror was mounted at a 45° angle at the bottom of the tank. Prior to each test, distilled water in the tank was mixed thoroughly and degassed by boiling for about 15 min. Also, the surface of the copper section was

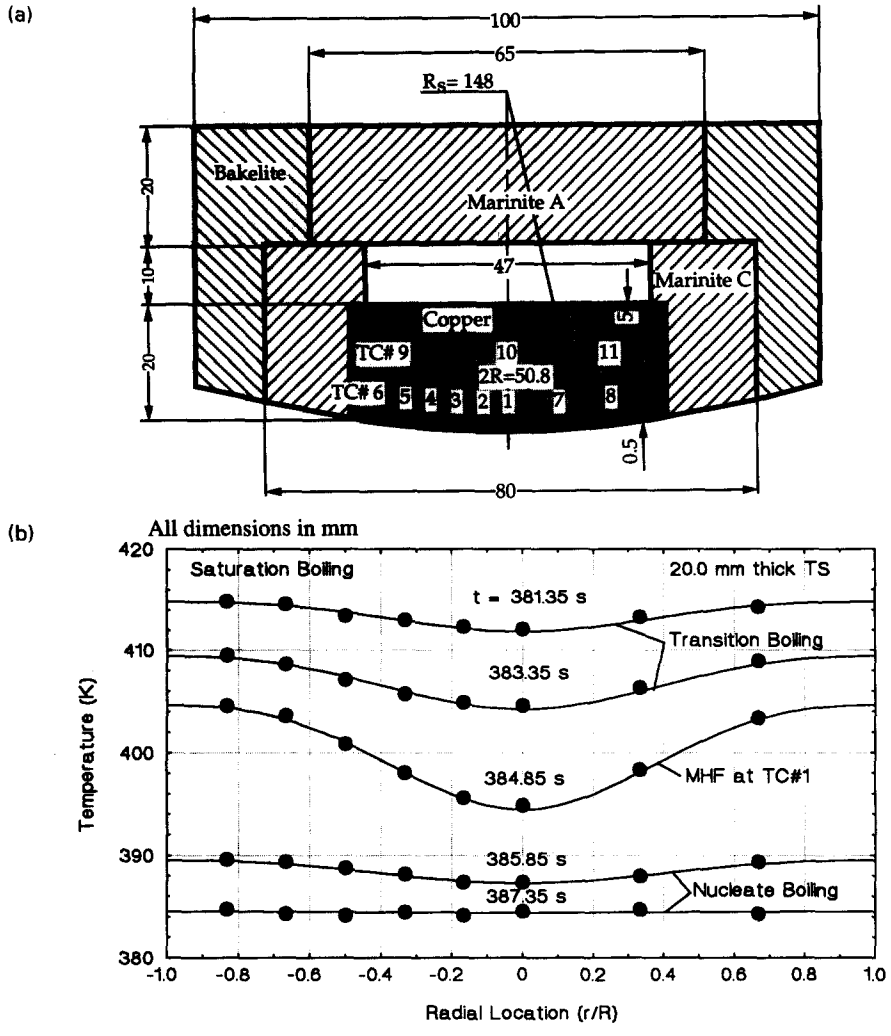

Fig. 1. (a) Cross-sectional view of instrumented test section. (b) Measured temperature distribution near the boiling surface during quenching.

polished using No. 1200 Silicon Carbide sand paper then cleaned with acetone. To avoid surface oxidization before quenching, the surface was wrapped in aluminum foil while being heated on a hot plate to about 510 K. The test section was then submerged into the water pool, ~40 mm below the surface. When the depth of water varied below 40 mm, the effect was negligible; larger depths were not considered, however, because of the small tank size.

During quenching, all thermocouples were scanned sequentially once every 100 ms and their recording time adjusted for the interval (~9 ms) between readings to obtain simultaneous temperature measurements. The raw temperature measurements had high frequency, random oscillations, due to electric equipment. In order to remove these oscillations without unduly degrading the underlying information, numerical filtering (or smoothing) of the raw temperature data was performed [8] using a method similar to that described in [12]. After numerical filtering, the measured temperatures near the boiling surface were used, in conjunction with a two-dimensional (r, z) transient solution of heat conduction in the copper section during quenching, to determine the local and average pool boiling heat fluxes and surface temperatures [7, 8].

Determination of pool boiling heat flux

The two-dimensional, transient heat conduction equation in the copper section was solved numerically using, as a boundary condition, the recorded temperatures near the boiling surface (TC1–TC8) during quenching [Fig. 1(b)], to derive the local surface heat fluxes and surface temperatures [7, 8]. The times listed in Fig. 1(b) are measured from the beginning of quenching in the saturation boiling experiments, starting at a wall superheat of 135 K. The numerical solution employed a fully implicit alternating direction, finite control volume (CV) method, (20×20) calculation grid, and a convergence coefficient of 10^{-6}. When a (30×30) grid and/or a smaller convergence coefficient were used, computation time increased sig-

nificantly with negligible changes in the calculated values of the pool boiling heat flux and surface temperature.

The temperatures within the copper section were calculated at the center and the heat flux at the boundaries of the control volumes. The local heat flow at the boiling surface was determined from the heat balance in the control volumes (CVs) bounded by the boiling surface. The local pool boiling heat flux was then determined by dividing the calculated heat flow by the corresponding surface area of the control volume. The local surface temperatures were determined from the parabolic extrapolation of the calculated temperatures at centers of CVs in the three rows near the boiling surface. The surface average pool boiling heat flux was determined by dividing the calculated total heat flow from the boiling surface by the total surface area. The average wall temperature was determined from the integral of the local wall temperatures over the entire boiling surface. The error in numerical calculations, determined from the overall energy balance after each time interval, was less than 1.0%, and the difference between calculated and measured temperatures by TC9–TC11 was about ± 0.5 K. The overall uncertainties in the local and average film boiling heat flux, determined using the method outlined in [13], were $\pm 9\%$ and $\pm 4\%$, respectively. More details on the numerical solution are given in [14].

RESULTS AND DISCUSSION

Experimental results presented in this section show the effects of water subcooling on both local and surface average film boiling curves and the critical film thicknesses prior to surface rewetting. The local film boiling curves presented are the average of two separate tests performed at the same conditions to confirm the reproducibility of experimental results [7, 8]; results were reproducible to within $\pm 5\%$.

Visual observations

Visual observations and video images of film boiling revealed that the surface was covered initially by a stable vapor film [Figs. 2(a), 3(a) and 4(a)]. The destabilization and collapse of film boiling, resulting in surface rewetting, were hydrodynamically driven in saturation boiling [Figs. 2(b), 4(c) and 4(d)], but thermally driven in subcooled boiling [Fig. 3(b)]. In saturation boiling, all the heat released from the surface was consumed in vapor generation. The vapor flow under the effect of tangential gravity component caused the film to be thinnest at the lowermost position and thickest near the edge [Fig. 4(a)]. At high wall superheat, intermittent releases of vapor from the periphery of the swelled film caused the vapor–liquid interface to oscillate repetitively [Figs. 2(b), 4(b) and 4(c)], then fully stabilize as excess vapor in the film was released [Figs. 2(a) and 4(a)]. The average volume of released vapor increased, but the release frequency decreased as the surface temperature decreased with time in film boiling. Eventually, film oscillations, following the release of vapor, destabilized film boiling, forcing surface rewetting [Figs. 2(c) and 4(d)].

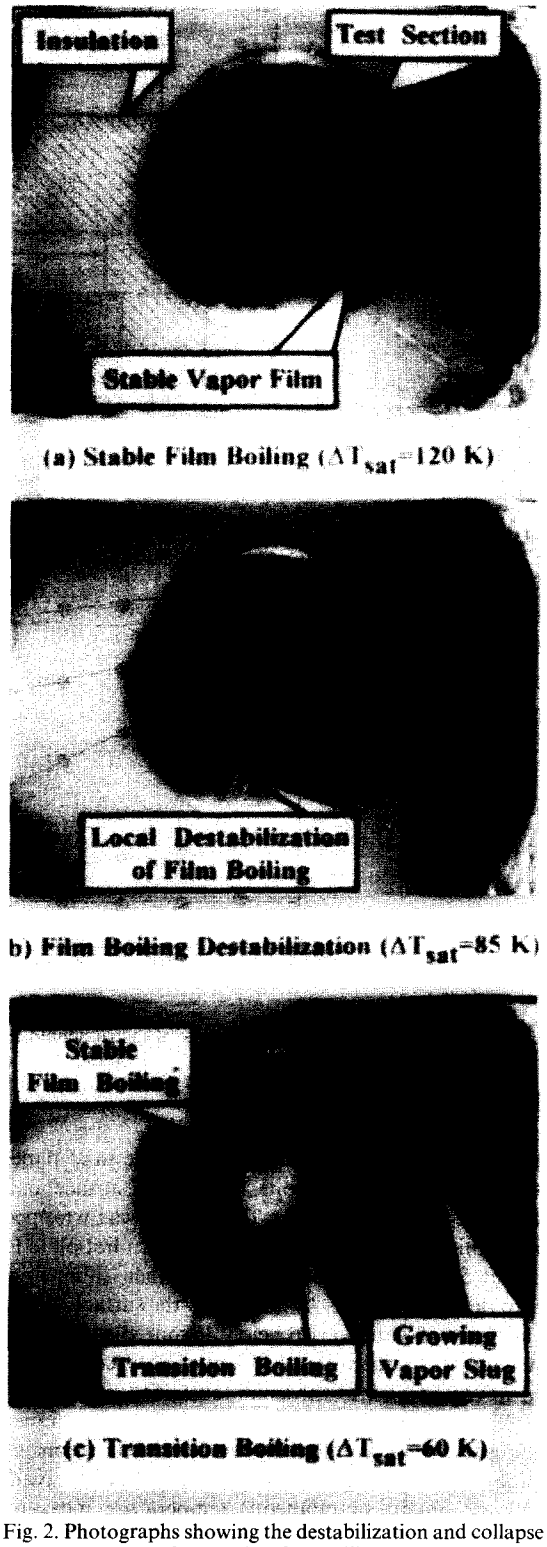

Fig. 2. Photographs showing the destabilization and collapse of saturation film boiling.

In subcooled boiling, however, only a fraction of

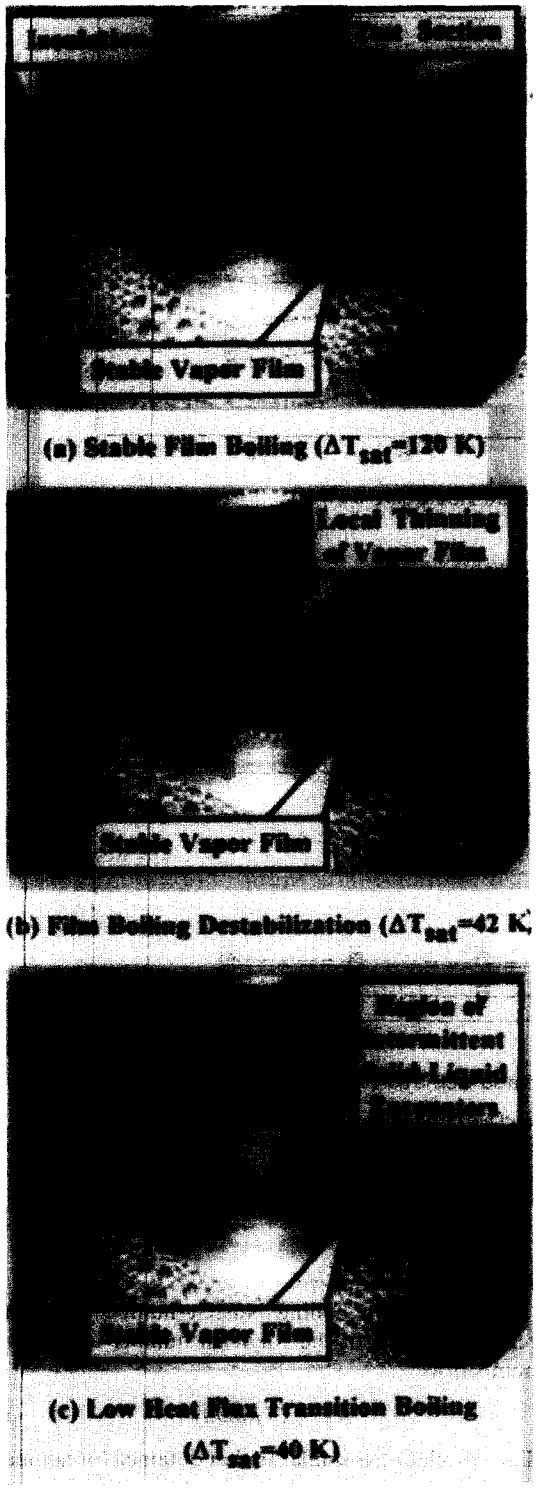

Fig. 3. Photographs showing the destabilization and collapse of subcooled film boiling.

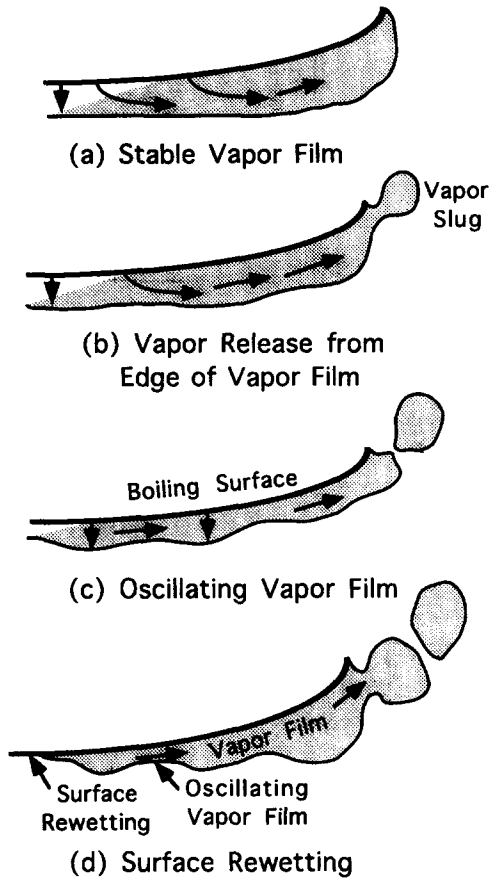

Fig. 4. Illustration of saturation film boiling on a downward-facing curved surface.

the heat released from the surface was consumed in vapor generation; the largest fraction was conducted through the vapor film to the underlying water pool to be removed by natural convection. Vapor generated at the lower positions on the surface accumulated at higher locations, increasing the film thickness. At 10 and 14 K water subcooling, no vapor was seen released from the periphery of the vapor film. At 5 K subcooling, however, vapor release from the edge of vapor film only occurred at high wall superheat [Figs. 3(a) and 4(a)]. As the surface temperature dropped, less vapor was generated and the film thickness continued to decrease due to condensation. Eventually, the vapor film in the inner portion of the surface, where it is thinnest, collapsed locally [Fig. 3(b)], then surface rewetting propagated radially outward.

As indicated later, the rewetting time (or duration of film boiling) of ~273 s in saturation boiling was much shorter than in subcooled boiling (415 s–678 s). In subcooled boiling, the decrease in rewetting time with increased water subcooling, resulted in smaller film thickness prior to rewetting, but higher minimum film boiling heat flux. In transition boiling, vapor nucleation in the inner portion of the surface was more coarse [Fig. 2(c)] than in subcooled boiling [Fig. 3(c)]. Also, transition boiling was accompanied by frequent vapor release from the edge of the copper surface [Fig. 2(c)]. In subcooled boiling no vapor release was observed at the beginning of transition boiling at high wall superheat [Fig. 3(c)].

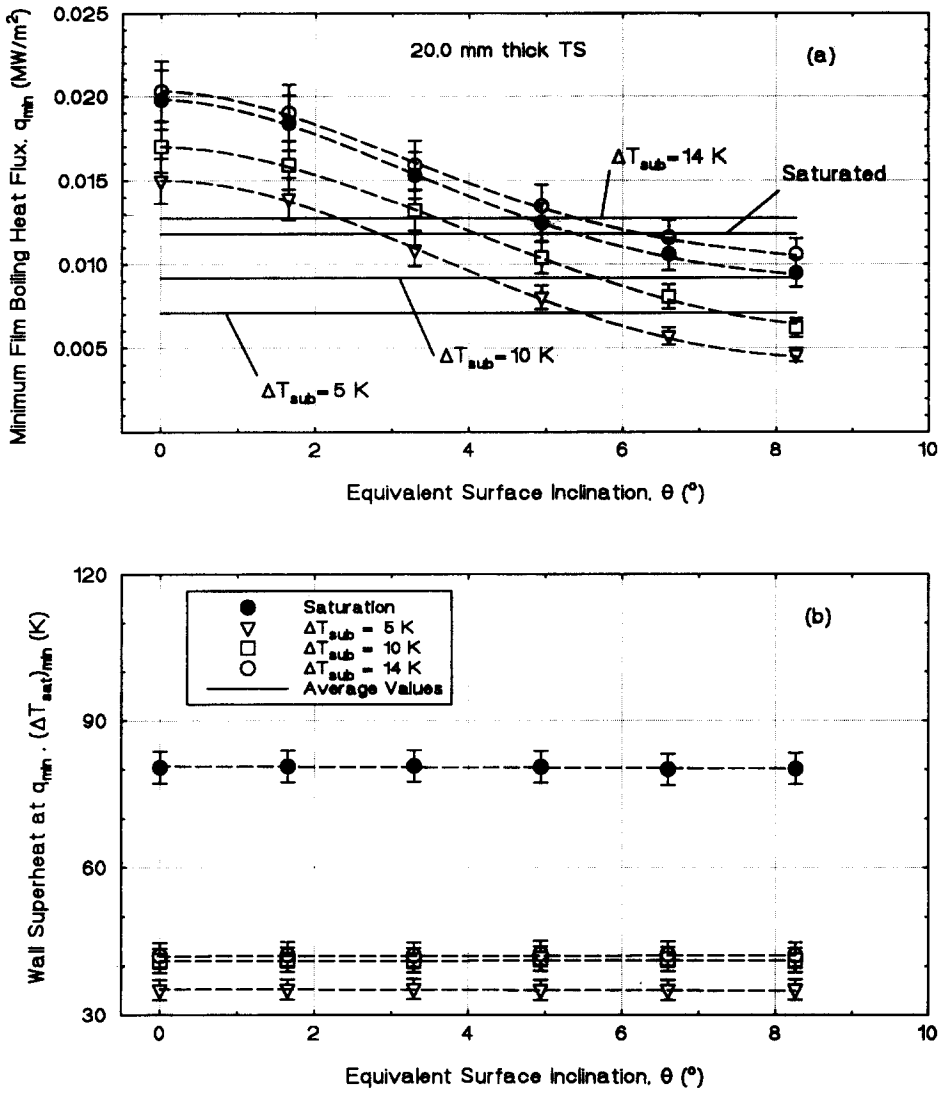

Fig. 5. Minimum film boiling heat flux and corresponding wall superheat.

Minimum pool boiling

Figures 5(a) and (b) show that q_{min} and $(\Delta T_{sat})_{min}$ both increased with increased subcooling; higher water subcooling caused film boiling to quench earlier. The minimum film boiling heat flux also increased with decreased inclination, θ. The values $(\Delta T_{sat})_{min}$, however, were independent of θ because the high thermal conductivity of the copper stimulated lateral conduction near the surface, resulting in a uniform surface temperature [Fig. 5(b)]. In saturation boiling, the minimum film boiling heat flux was significantly higher than that at 5 and 10 K subcooling, but only slightly lower than that at 14 K subcooling. As indicated earlier, because film boiling destabilization in saturation boiling was hydrodynamically driven, surface rewetting occurred earlier, at both higher heat flux and wall superheat.

Film boiling correlations

The local film boiling Nusselt number was correlated in terms of the Rayleigh number and Jacob numbers as:

$$Nu = C(Ra/Ja)^a. \quad (1)$$

This correlation is similar to that obtained for laminar film boiling on an isothermal sphere using integral boundary layer analysis [15], except that the coefficient "C" and the exponent "a" are functions of θ as follows:

$$C = \exp(C_1 \cdot \theta + C_2), \quad (2)$$

and,

$$a = a_1 \cdot \theta + a_2. \quad (3)$$

For saturation boiling, these coefficient are: $C_1 =$

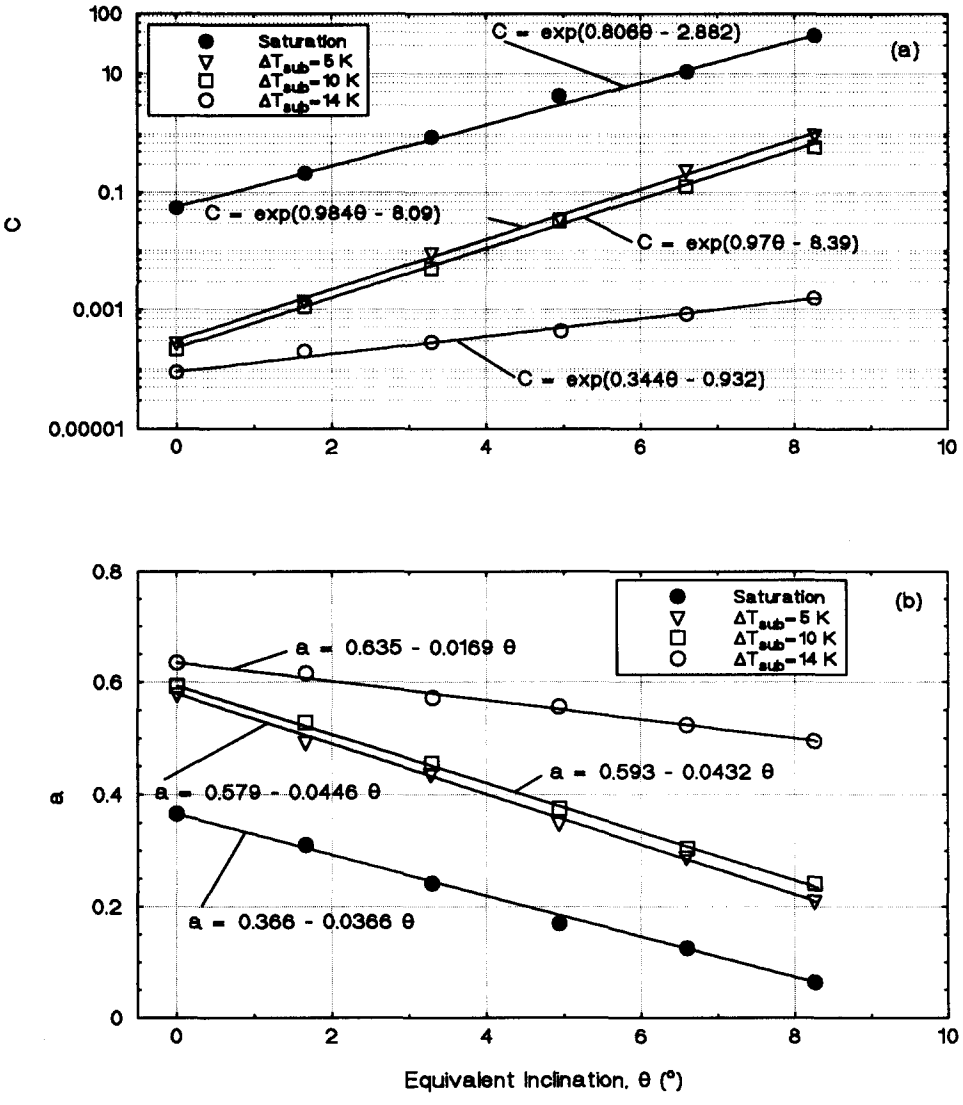

Fig. 6. Nusselt number correlation coefficients for film boiling.

0.806, $C_2 = -2.882$, $a_1 = -0.0366$ and $a_2 = 0.366$. For water subcooling, $5\ \text{K} \leqslant \Delta T_{sub} \leqslant 14\ \text{K}$, these coefficients were correlated as follows:

$$C_1 = 0.984 - 1.02 \times 10^{-6} \exp(0.954 \Delta T_{sub}) \quad (4)$$

$$C_2 = -8.0 - 1.74 \times 10^{-2} \exp(0.31 \Delta T_{sub}) \quad (5)$$

$$a_1 = -0.045 + 8.75 \times 10^{-7} \exp(0.74 \Delta T_{sub}) \quad (6)$$

$$a_2 = -0.575 + 8.865 \times 10^{-4} \exp(0.30 \Delta T_{sub}). \quad (7)$$

As shown in Figs. 6(a) and (b) the coefficient "C" [equation (2)] increased with increased inclination angle, but decreased with increased subcooling [Fig. 6(a)]. Conversely, the exponent "a" in equation (1) decreased with increased inclination, but increased with increased water subcooling [Fig. 6(b)]. Figure 7(a) shows that the correlation for the local Nusselt number, equation (1), is within $\pm 10\%$ of the data. Note that the validity of equation (1) is limited to the present data for which $\Delta T_{sub} < 14$ K.

Similarly, the surface average Nusselt number for saturation and subcooled boiling ($\Delta T_{sub} < 14$ K) was correlated as

$$\bar{N}u = B(Ra/\bar{J}a)^b \quad (8)$$

where, $B = 4.8$ and $b = 0.162$ for saturation film boiling. For subcooled boiling, the coefficient B and the exponent b are

$$B = 6.53 \times 10^{-2} - 3.93 \times 10^{-3} \exp(0.20 \Delta T_{sub}) \quad (9)$$

$$b = 0.34 + 1.66 \times 10^{-4} \exp(0.506 \Delta T_{sub}). \quad (10)$$

As shown in Fig. 7(b), the correlation of the average film boiling Nusselt number [equation (8)] is in agreement with experimental data to within $\pm 5\%$.

Rewetting time

As shown in Figs. 5 and 8, there is a direct correlation between the values of both q_{min} and $(\Delta T_{sat})_{min}$ and the rewetting time. Figure 5(a) and the insert in

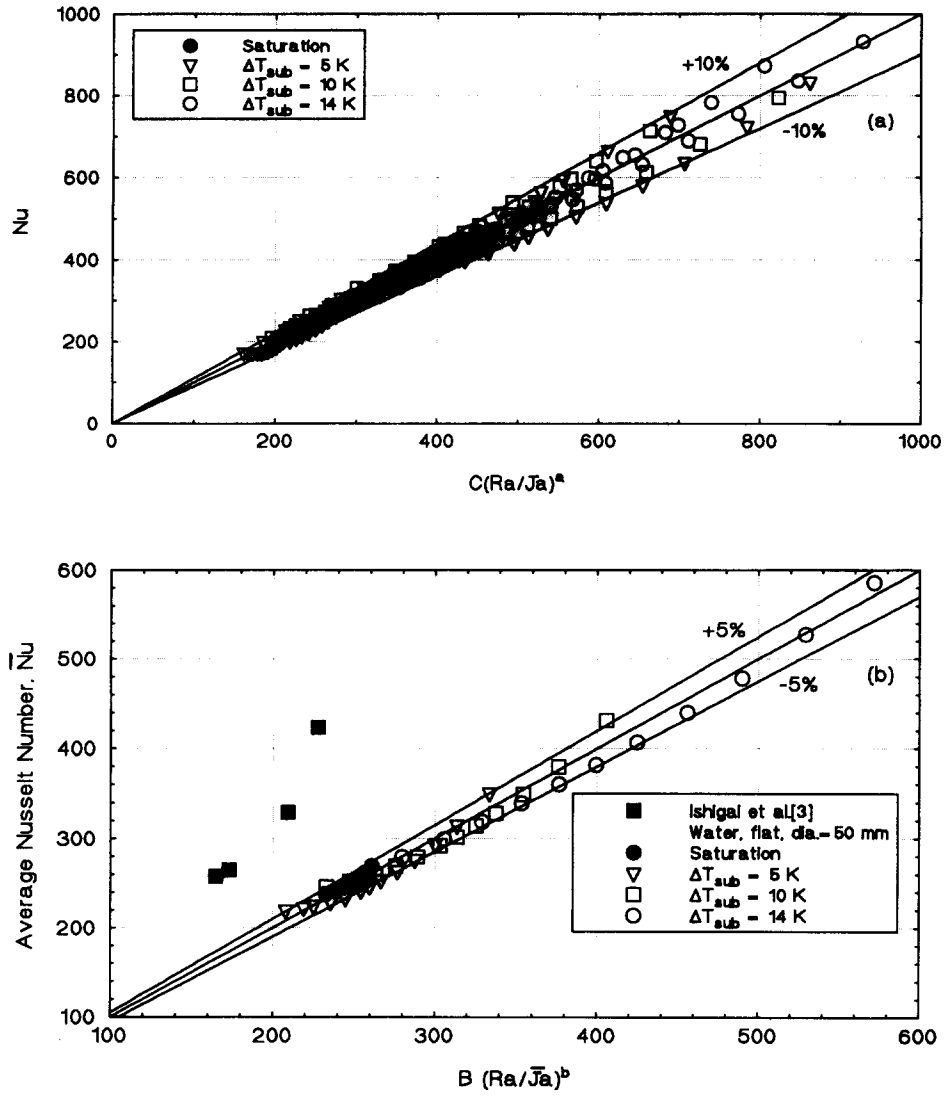

Fig. 7. (a) Nusselt number correlation for local film boiling heat transfer. (b) Nusselt number correlation for surface average film boiling heat transfer.

Fig. 8(a) show that in subcooled boiling lower q_{min} and $(\Delta T_{sat})_{min}$ were always associated with longer rewetting time. Unlike q_{min}, the rewetting time increased as the local inclination on the boiling surface, θ, increased or water subcooling decreased. The insert in Fig. 8(a) compares the rewetting time measured for the lowermost position ($\theta = 0^\circ$) at saturation and at different water subcooling. The smallest rewetting time of 273 s was for saturation film boiling, followed by that for 14 K subcooling (415 s), then increased to 506 s and 678 s at 10 K and 5 K subcooling, respectively. These times were measured in experiments starting at a wall superheat of 135 K.

In order to examine the progression of rewetting on the surface, the rewetting time is normalized to that at the lowermost position and results plotted in Fig. 8(a). The slowest progression of surface rewetting occurred at saturation and the fastest at 14 K subcooling. For example, in saturation film boiling surface rewetting at $\theta = 8.26^\circ$ occurred about 285 ms after the lowermost position ($\theta = 0^\circ$). At 14 K subcooling, however, surface rewetting at the same location occurred only about 115 ms after the lowermost position.

Determination of film thickness and volume of released vapor

During film boiling, thermal energy is transferred from the metal section surface to the liquid–vapor interface by conduction and radiation; convection is negligible due to the low vapor flow relative to the surface. Because the initial surface temperature at quenching (~ 513 K) and the emissivity of copper (0.1) are relatively low, the radiation contribution was small compared to that by conduction. Therefore, the average vapor film thickness in film boiling can be expressed as [17]:

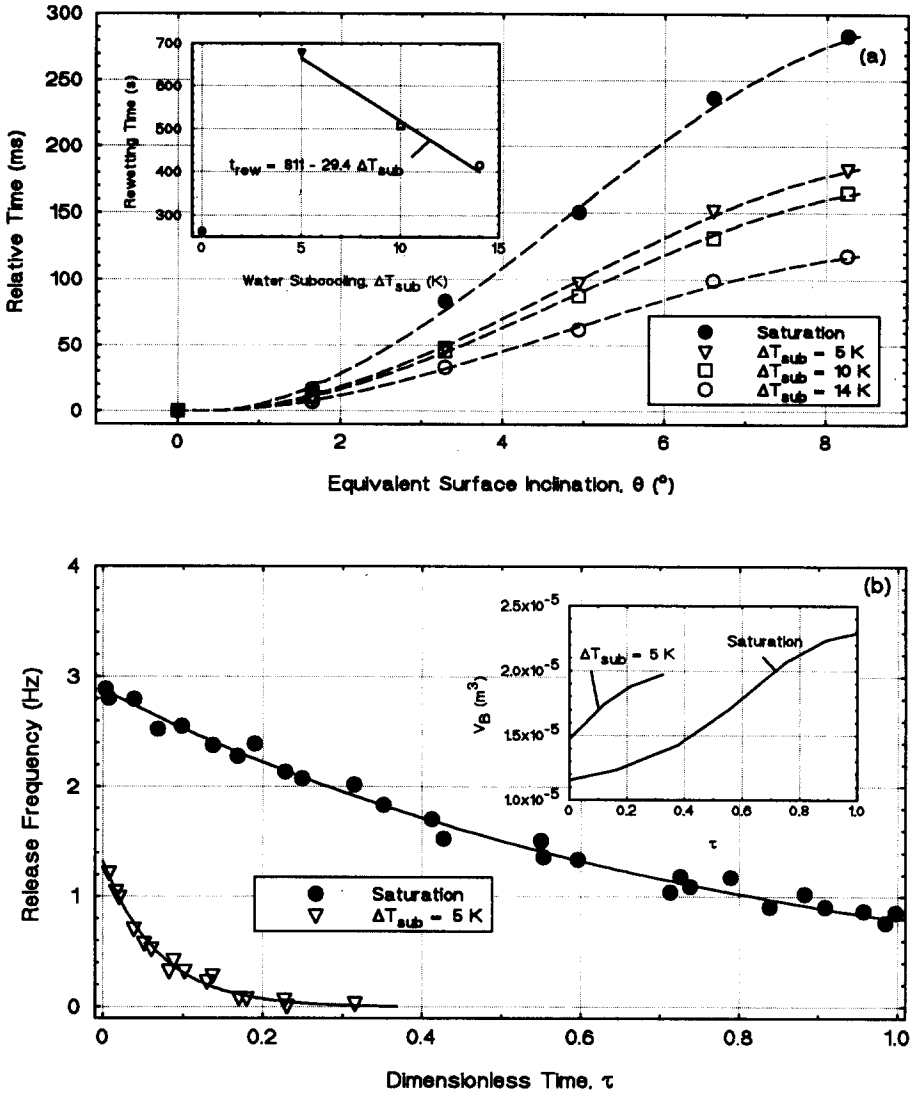

Fig. 8. (a) Rewetting time for saturation and subcooled film boiling. (b) Vapor release frequency and volume in film boiling.

$$\bar{\delta}_{fB}(t) = k_v/[\bar{h}_{fB} - 0.75\bar{h}_R] \quad (11)$$

where,

$$\bar{h}_{fB} = (\bar{N}u \cdot k_v/D) \quad (12)$$

$$\bar{h}_R = \varepsilon\sigma(\bar{T}_w^4 - T_{sat}^4)/\Delta\bar{T}_{sat} \quad (13)$$

and,

$$\varepsilon = \{1/\varepsilon_w + 1/\varepsilon_l - 1\}^{-1}. \quad (14)$$

In equation (14), the water emissivity, ε_l, was taken equal to 0.95. The local film thickness can also be expressed in terms of the local heat transfer coefficients as

$$\delta_{fB}(\theta, t) = k_v/(h_{fB} - 0.75h_R) \quad (15)$$

where, h_{fB} and h_R are the local film boiling and radiation heat transfer coefficients, respectively. Equation (15) applies between releases of vapor from the edge of the boiling surface. The average volume of released vapor, $V_B(t)$, is determined from the mass balance

$$V_B f\rho_v = (\bar{q}_{ev}A/h'_{fg}) + \rho_v A(d\bar{\delta}_{fB}/dt). \quad (16)$$

Since the average film thickness changes slowly with time, the second term on the right hand side of equation (16) is negligible compared to the first term, thus

$$V_B(t) = [(\bar{q}_{ev}A)/(f\rho_v h'_{fg})] \quad (17)$$

where,

$$\bar{q}_{ev} = \bar{h}_{fB}\Delta\bar{T}_{sat} - \bar{h}_{NC}\Delta\bar{T}_{sub}. \quad (18)$$

The natural convection heat transfer coefficient from the vapor–liquid interface to the underlying subcooled liquid pool is determined from the following correlation for a heated, downward-facing flat surface [18]

$$\bar{h}_{NC} = 0.27(k_f/D)[(\beta g \Delta \bar{T}_{sub} D^3)/\nu_f \alpha_f]^{0.25}. \quad (19)$$

Equation (17) is rearranged to give the following general expression for V_B

$$V_B(t) = B\bar{J}a(Ra/\bar{J}a)^b[A\alpha_v/(Df)] - [\bar{h}_{NC} A \Delta \bar{T}_{sub}/(f\rho_v h'_{fg})]. \quad (20)$$

In saturation boiling, the second term on the right hand side of equation (20) drops out, thus:

$$V_{B_{sat}}(t) = B\bar{J}a(Ra/\bar{J}a)^b[A\alpha_v/(Df)]. \quad (21)$$

In equations (20) and (21), the vapor release frequency is determined from the video images of the boiling surface during quenching. The video recording speed was about 60 field s^{-1}, thus the reported frequencies in Fig. 8(b) are accurate to within 0.016 Hz. As indicated earlier and shown in Fig. 8(b), at 5 K subcooling, intermittent release of vapor from the edge of the vapor film was only observed at high wall superheat ($\Delta T_{sat} > 105$ K). In saturation boiling, however, vapor release continued until surface rewetting occurred. The insert in Fig. 8(b) presents estimates of vapor release volume for saturation and 5 K subcooling. At 5 K subcooling, while the average volume of released vapor was larger, the release frequency was lower than at saturation. The vapor release frequency for 5 K subcooled boiling was significantly lower than that for saturation film boiling. In saturation film boiling, the vapor release frequency decreased from ~ 2.9 Hz at the beginning of film boiling (at wall superheat of 135 K) to about 0.8 Hz prior to rewetting at $\Delta T_{sat} \sim 80$ K [Fig. 8(b)]. The vapor release frequency at 5 K subcooling decreased from an initial value of ~ 1.2 Hz to zero at $\tau = 0.4$; a dimensionless time, τ, of unity corresponds to surface rewetting.

Film boiling curves

Figures 9(a)–(d) compare the experimental values of local (at three locations) and surface average film boiling curves for saturation and 5, 10 and 14 K subcooling. The minimum film boiling heat flux at 14 K subcooling was higher than at saturation, while $(\Delta T_{sat})_{min}$ for saturation boiling was higher than at 14 K subcooling. For lower subcooling, the values of q_{min} and $(\Delta T_{sat})_{min}$ as well as of the film boiling heat flux were much lower and increased with increased water subcooling. The values of q_{min} also increased with decreased inclination on the surface, $(\Delta T_{sat})_{min}$, however, were independent of local inclination (Figs. 5 and 9). The film boiling heat flux also increased with decreased inclination due to the reduction in film thickness.

Vapor film thickness

Figures 10(a)–(d) show the dependence of film thickness, calculated from equation (15), on wall superheat at four different locations on the surface, at saturation and 5, 10 and 14 K subcooling. The film thickness all along the surface decreased with increased water subcooling, but increased with increased inclination due to vapor accumulation. For example, at $\Delta T_{sat} = 100$ K, the vapor film thickness for 14 K subcooling increased from ~ 90 μm at $\theta = 0°$ to ~ 160 μm at $\theta = 8.26°$. At lower subcooling, the rate of heat removal by natural convection from the vapor film decreased, causing the film thickness to initially increase. At 5 and 10 K subcooling, the film swelled significantly at higher locations due to the accumulation of vapor generated at lower positions. The film thickness increased with decreased wall superheat, reaching a maximum when the rate of heat release from the surface became equal to that removed by natural convection from the vapor–liquid interface. Beyond this point, film thickness decreased, as the wall superheat decreased, due to condensation. Figures 10(a)–(d) show that at $\theta = 8.26°$ and 5 K subcooling, the maximum film thickness of ~ 280 μm occurred at a wall superheat of 75 K. At higher subcooling of 10 K, this film thickness decreased to ~ 240 μm and occurred at a higher wall superheat of ~ 90 K [Fig. 10(d)]. At 14 K subcooling, no swelling of the vapor film occurred because of the relatively higher rate of heat removal from the film by natural convection in the water pool. Eventually, surface rewetting occurred when the film thickness reached a critical value, which was dependent on water subcooling and local inclination on the boiling surface. Because of the intermittent vapor release in saturation film boiling, the swelling of the vapor film was negligible compared to that which occurred at 5 and 10 K subcooling [Figs. 10(a)–(d)].

Figures 11(a)–(g) show the vapor film thickness profiles, calculated from equation (15) for 5, 10 and 14 K subcooling, at wall superheats of 130, 115, 100, 85, 70, 60 and 50 K and at the minimum film boiling (or surface rewetting), respectively. For all wall superheats and water subcoolings, the vapor film thickness was lowest at the lowermost position on the surface and increased in the direction of vapor flow toward the edge of the copper surface. At $\Delta T_{sat} = 130$ K, the film thickness for all values of water subcooling investigated was almost the same at the lowermost position, but increased with decreased subcooling at higher inclination on the surface. As ΔT_{sat} decreased to 70 K, the difference in film thickness due to water subcooling increased. Further decrease in ΔT_{sat} caused the values of the vapor film thickness for 5, 10 and 14 K subcooling to decrease and become closer.

Critical vapor film thickness

As indicated in Figs. 10(a)–(d), in saturation boiling at the lowermost position on the surface ($\theta = 0°$), the critical film thickness prior to rewetting, δ_c, is $\sim 50 \pm 5$ μm, and almost independent of water subcooling. This film thickness, however, increased with increased inclination on the surface, but with decreased water subcooling. For instance, at $\theta = 8.26°$, δ_c increased to ~ 104, 140 and 175 μm at

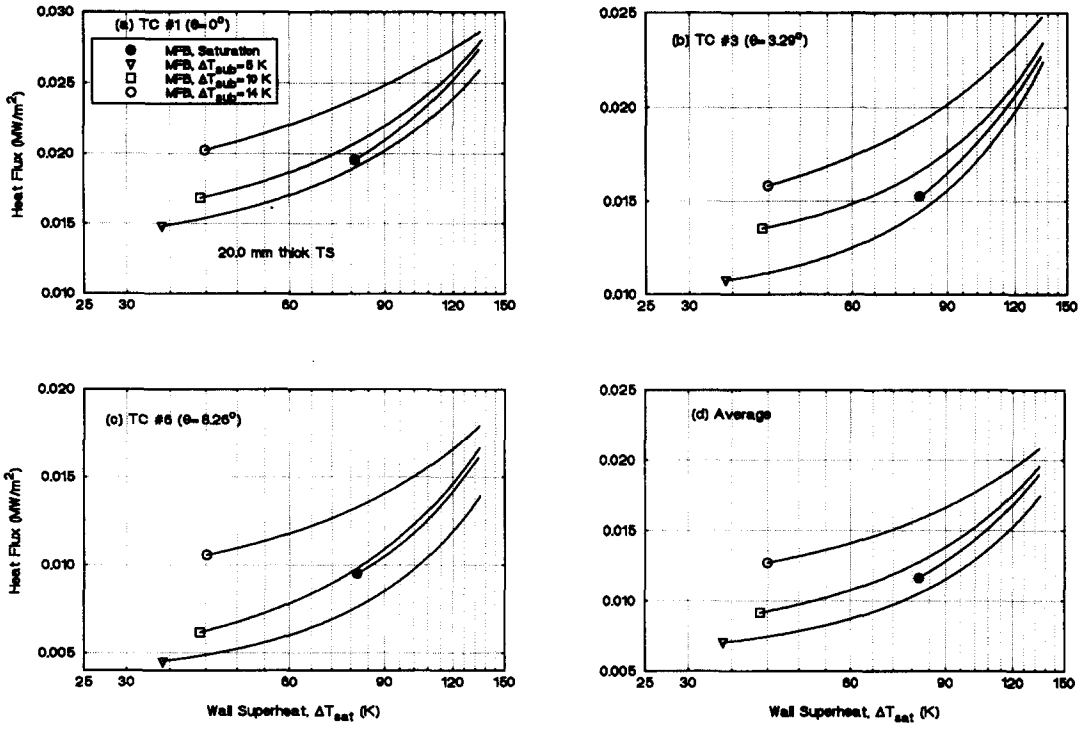

Fig. 9. Local and surface average film boiling curves.

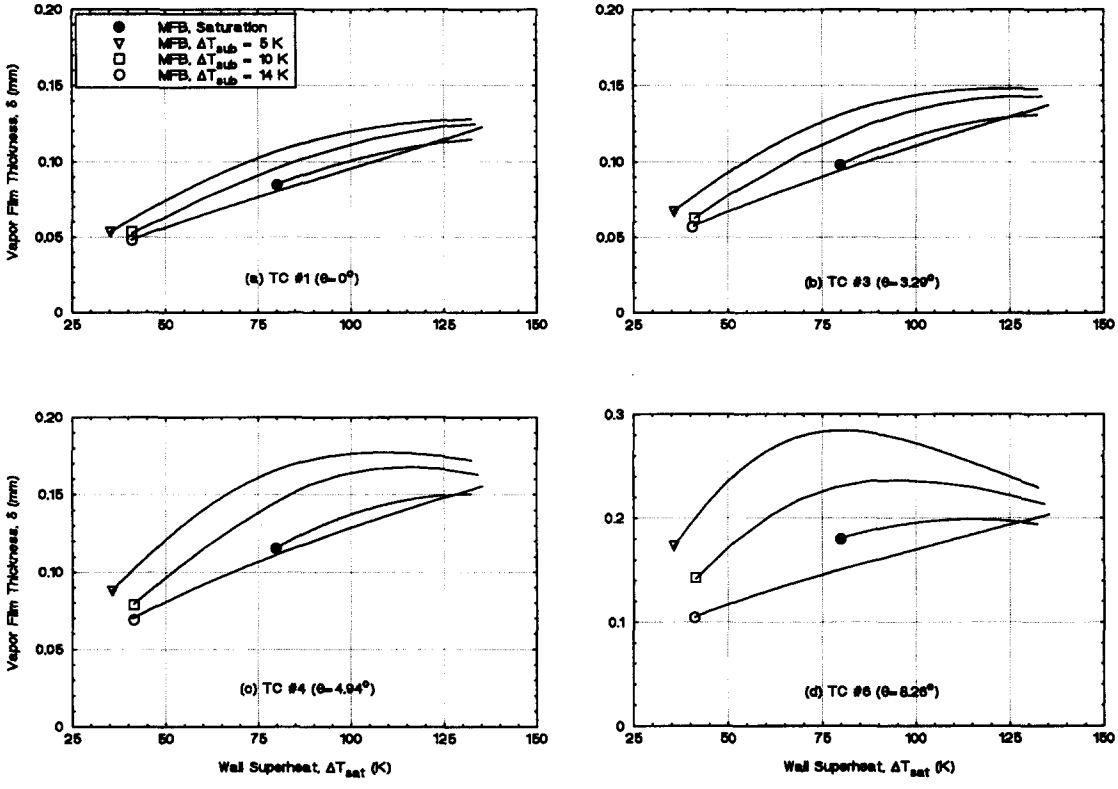

Fig. 10. Calculated vapor film thickness in saturation and subcooled boiling.

water subcooling of 14, 10 and 5 K, respectively [Figs. 11(h) and 12].

As delineated in Figs. 8(a), 10–12, in saturation boiling rewetting at the respective locations on the surface occurred at high wall superheats, δ_c, however, was higher than those for 5, 10 and 14 K subcooling.

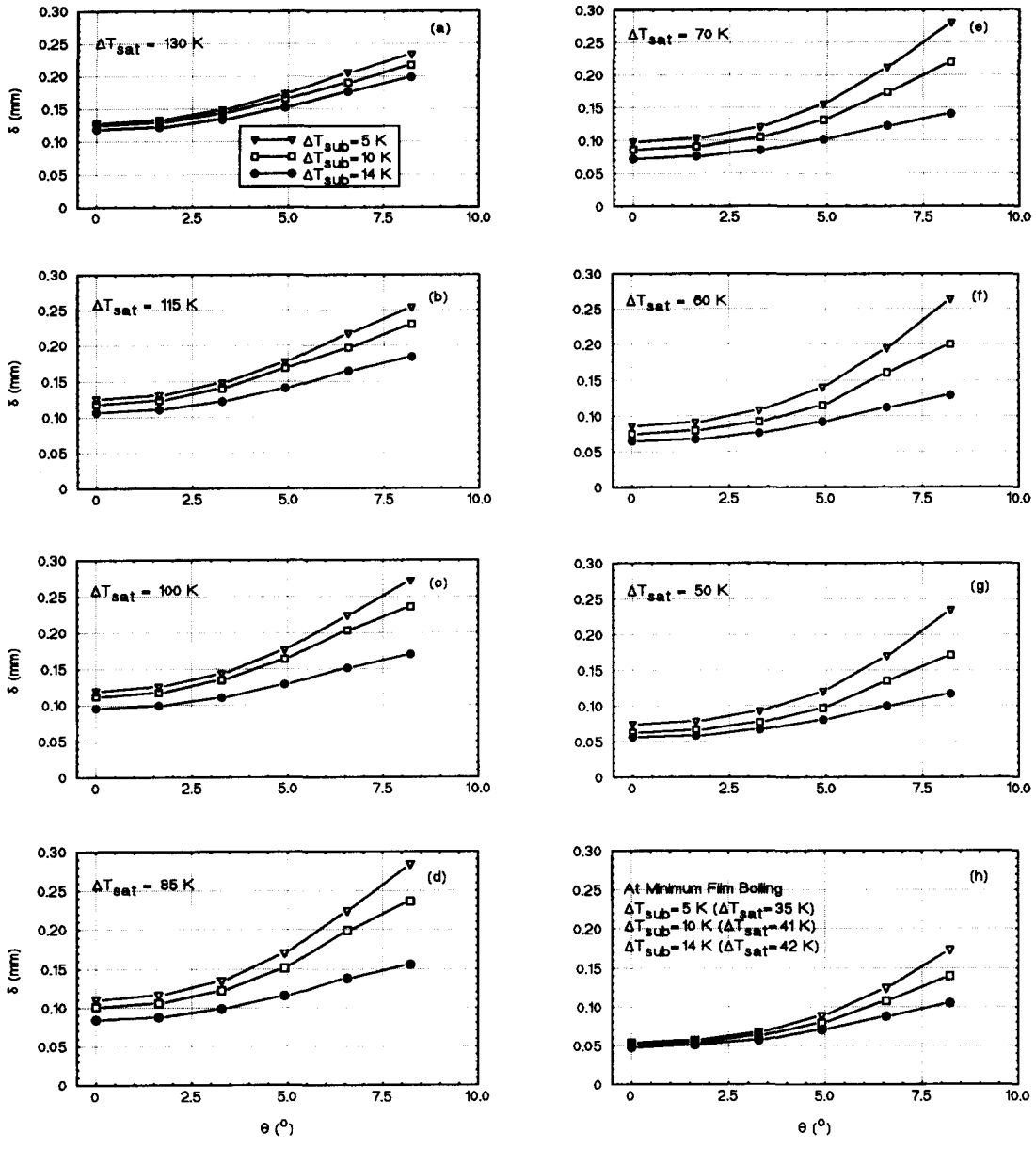

Fig. 11. Angular distribution of vapor film thickness in saturation boiling.

For saturation and subcooled boiling, δ_c increased with increased inclination on the surface. For example, δ_c for saturation boiling increased from ~ 85 μm at $\theta = 0^\circ$ to as much as 180 μm at $\theta = 8.26^\circ$. At $\theta = 8.26^\circ$, δ_c for 14, 10 and 5 K subcooling was ~ 104, 140 and 175 μm, respectively. Figure 12 also shows that the difference between δ_c values at various inclinations on the surface decreased with increased subcooling. The present results confirm the critical vapor film thickness concept [16, 19, 20] for rewetting in pool boiling from downward-facing surfaces. Figure 12 shows that the values of δ_c for $\theta < 4.94^\circ$ at saturation to $\theta < 6.6^\circ$ at 14 K subcooling, lie between the predictions of the wave theory of Chang [20] and the hydrodynamic instability theory of Berenson [18] for film boiling on a flat plate facing upward. At higher surface inclinations, the present values of δ_c are higher than that predicted by the hydrodynamic theory [19]. The lower the inclination angle, however, the closer are the present values of the critical film thickness to the predictions based on the wave theory [20].

SUMMARY AND CONCLUSIONS

Film boiling heat transfer from a downward-facing curved surface in saturated and 5, 10 and 14 K subcooled water was investigated. The local and surface

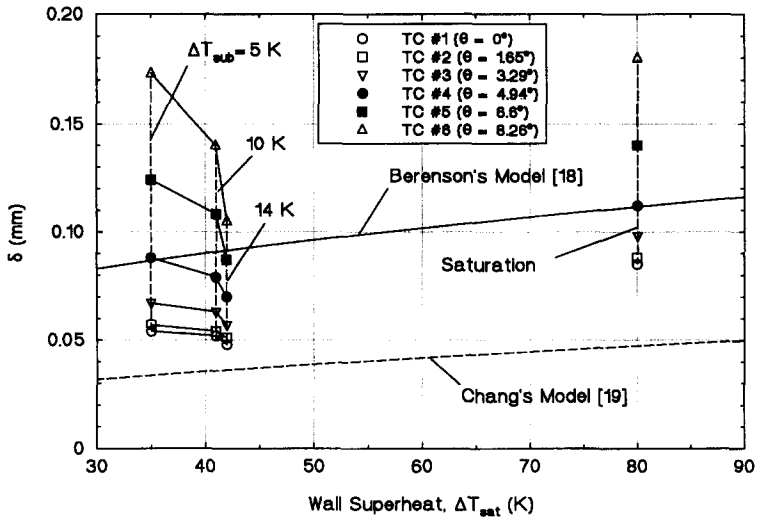

Fig. 12. Critical vapor film thickness for surface rewetting.

average Nusselt numbers were correlated in terms of the Rayleigh and Jacob numbers, for both saturation and subcooling conditions; the correlations were in good agreement with the data to within $\pm 10\%$ and $\pm 5\%$, respectively.

In saturation film boiling, the rewetting time (~ 273 s) was much shorter than in subcooled boiling (415 s–678 s). The decrease in rewetting time with increased water subcooling, resulted in a smaller critical film thickness and, hence, higher minimum film boiling heat flux and corresponding wall superheat. Results demonstrated a direct correlation between the values of both q_{min} and $(\Delta T_{sat})_{min}$ and rewetting time. Lower q_{min} and $(\Delta T_{sat})_{min}$ were always associated with longer rewetting time and larger δ_c. The rewetting time and δ_c increased as either the local inclination on the boiling surface, θ, increased or water subcooling decreased. The values of q_{min} and $(\Delta T_{sat})_{min}$ both increased with increased subcooling. The film boiling heat flux also increased with decreased inclination, while $(\Delta T_{sat})_{min}$ was independent of surface inclination.

The shortest film boiling duration in saturation boiling was caused by early collapse of vapor film and rewetting of the surface, triggered by the oscillations (or hydrodynamic instability) induced by vapor release from the edge of the film. In subcooled boiling, however, the collapse of the vapor film and rewetting of the surface were thermally driven. Surface rewetting occurred first at the lowermost position, $\theta = 0°$, then sequentially at higher inclination positions. For saturation boiling, δ_c was 85 μm at $\theta = 0°$, increasing to 180 μm at $\theta = 8.26°$. For subcooled boiling at $\theta = 0°$, the critical film thickness (~ 50 μm) was smaller and weakly dependent on subcooling; it increased, however, with increased inclination and decreased subcooling, reaching ~ 175 μm at $\theta = 8.26°$ and 5 K subcooling.

The critical film thickness for $\theta < 4.94°$ at saturation to $\theta < 6.6°$ at 14 K subcooling, fell between the predictions of the wave and the hydrodynamic instability theories for film boiling on a flat plate facing upward. The critical film thickness at higher surface inclinations were larger than predicted by the hydrodynamic theory. At lower inclination, however, the critical film thickness were closer to the predictions of the wave theory.

Acknowledgements—Research sponsored by the Institute for Space and Nuclear Power Studies, University of New Mexico, Albuquerque, NM.

REFERENCES

1. S. Ishigai, K. Inoue, Z. Kiwaki and T. Inai, Boiling heat transfer from a flat surface facing downward, *Proc. Int. Heat Trans. Conf*, Paper No. 26 (1961).
2. D. S. Jung, J. E. S. Venart and A. C. M. Sousa, Effects of enhanced surfaces and surface orientation on nucleate and film boiling heat transfer in R-11, *Int. J. Heat Mass Transfer* **30**(12), 2627–2639 (1987).
3. N. Seki, S. Fukushako and K. Torikoshi, Experimental study on the effect of orientation of heating circular plate on film boiling heat transfer for fluorocarbon refrigerant R-11, *J. Heat Transfer* **100**, 624–628 (1978).
4. Z. Guo and M. S. El-Genk, An experimental study of saturated pool boiling from downward facing and inclined surfaces, *Int. J. Heat Mass Transfer* **35**(9), 2109–2117 (1992).
5. Z. Guo and M. S. El-Genk, Effects of liquid subcooling on the quenching of inclined and downward-facing flat surfaces in water, *A.I.Ch.E. Symp. Ser.* **288**(88), 241–248 (1992).
6. M. S. El-Genk and Z. Guo, Transient boiling from inclined and downward-facing surfaces in a saturated pool, *Int. J. Refrig.* **16**(6), 414–422 (1993).
7. M. S. El-Genk, A. G. Glebov and Z. Guo, Pool boiling from downward-facing curved surface in saturated water, *Proc. 10th Int. Heat Trans. Conf.*, Brighton, Vol. 5, pp. 45–50 (1994).
8. M. S. El-Genk and A. G. Glebov, Transient pool boiling from downward-facing curved surfaces, *Int. J. Heat Mass Transfer* **38**, 2209–2224 (1995).
9. J. E. O'Brien and G. L. Hawkes, Thermal analysis of a reactor lower head with core relocation and external

boiling heat transfer, *AIChE Symp. Ser.* **283**(87), 159–168 (1991).
10. H. Park and V. K. Dhir, Steady-state thermal analysis of external cooling of a PWR vessel lower head, *A.I.Ch.E. Symp. Ser.* **283**(87), 1–7 (1991).
11. R. E. Henry, J. P. Burelbach, R. J. Hammersley, C. E. Henry and G. T. Klopp, Cooling of core debris within the reactor vessel lower head, *J. Nucl. Technol.* **101,** 385–399 (1993).
12. A. Savitzky and M. J. E. Golay, Smoothing and differentiation of data by simplified least square procedures, *Anal. Chem.* **36,** 1627–1639 (1964).
13. M. Kline and F. A. McClintock, Describing uncertainties in single-sample experiments, *Mech. Engng* (3–8 January 1953).
14. M. S. El-Genk and A. G. Glebov, Numerical solution of transient heat conduction in a cylindrical section during quenching, *J. Numer. Heat Transfer, Part-B: Applications* (in press).
15. V. P. Carey, *Liquid–Vapor Phase-Change Phenomena*, Chap. 7, pp. 275–278 Hemisphere Washington, DC (1992).
16. A. Abdul-Razzak, M. Shoukri and A. M. C. Chan, Rewetting of hot horizontal tubes, *Nucl. Engng Design* **138,** 375–388 (1992).
17. J. A. Bromley, Heat transfer in stable film boiling, *Chem. Engng Prog.* **46**(5), 221–227 (1950).
18. W. H. McAdams, *Heat Transmission*, Chap. 7, p. 180. McGraw-Hill, New York (1954).
19. P. J. Berenson, Film-boiling heat transfer from a horizontal surface, *J. Heat Transfer* **83,** 351–358 (1961).
20. Y. P. Chang, Wave theory of heat transfer in film boiling, *J. Heat Transfer* 1–12 (1959).